The Intramolecular Dynamic Behavior of Tetraaryl Allyl Radicals

Kohji Watanabe

Laboratory of Solid State Chemistry, Institute for Chemical Research, Kyoto University, Uji, Kyoto 611

(Received November 29, 1974)

The electron spin resonance (ESR) and the electron nuclear double resonance (ENDOR) spectra of tetraaryl allyl radicals have been observed. A comparison of the ENDOR spectra of $\alpha,\alpha,\gamma,\gamma$-tetraphenyl allyl, α,α-diphenyl-γ,γ-dianisyl allyl, and $\alpha,\alpha,\gamma,\gamma$-tetraanisyl allyl revealed that the four aryl groups are not equivalent, but are apparently to be classified into two types with different conformations in their molecular frameworks. The molecular orbital calculations on the basis of this model have shown a fairly good agreement with the observed spectra. The temperature dependence of the ENDOR spectra at $-60\sim-110\ ^\circ\mathrm{C}$ were analyzed, assuming mutually different twisting angles for the allyl skeleton. The activation energy of the torsional vibration of the allyl skeleton is estimated to be about 2.5 kcal/mol. The ESR spectra of $\alpha,\alpha,\gamma,\gamma$-tetraphenyl allyl and α,α-diphenyl-γ,γ-diphenylene allyl change drastically with the temperature at around $+115\ ^\circ\mathrm{C}$ and show a marked line-width alternation effect. It is concluded from the results that the torsional vibration becomes vigorous with an increase in the temperature and that the allyl skeleton begins to rotate internally at high temperatures. The activation energy of the internal rotation of the allyl skeleton has been estimated to be about $15\sim20$ kcal/mol. The temperature-dependent hyperfine splitting of the methine proton has also been explained by assuming a model of the internal rotation of the allyl skeleton.

Anomalously large proton hyperfine splittings have often been observed for the radicals which possess twisted π-systems in their molecular frames.[1,2] The present author and his co-workers[3] also observed similar phenomena in the ESR spectra of the tetraaryl allyl radicals. Such an extraordinarily large proton hyperfine splitting can be successfully explained by the following modified McConnell relation:

$$A_\beta^\mathrm{H} = |Q_\mathrm{CH}^\mathrm{H}|\cdot\rho_{\mathrm{C}\beta} + |B_{t-\pi}^\mathrm{H}|\{\cos^2(90-\theta)\cdot\rho_{\mathrm{C}\alpha}$$
$$+ \cos^2(90-\phi)\cdot\rho_{\mathrm{C}\gamma}\} \tag{1}$$

where Q_CH^H is $-22.5\sim-29.0$ G and where $\rho_{\mathrm{C}\alpha}$, $\rho_{\mathrm{C}\beta}$, and $\rho_{\mathrm{C}\gamma}$ are the $2p\pi$ spin densities on the α-carbon ($\mathrm{C}\alpha$), β-carbon ($\mathrm{C}\beta$), and γ-carbon ($\mathrm{C}\gamma$) atoms respectively. Here, $\mathrm{C}\alpha$ and $\mathrm{C}\gamma$ are the carbon atoms on the two sides of $\mathrm{C}\beta$ in the allyl molecule, and $B_{t-\pi}^\mathrm{H}$ is a proportionality constant for the twisted π-radical, where the magnitude of B^H for the neutral radical is usually estimated to be $50\sim60$ G.[4-6] The θ and ϕ angles are the mean values of the twisting angles of the $2p_z$-*orbitals* on $\mathrm{C}\alpha$ and $\mathrm{C}\gamma$ respectively. From Eq. (1) and McLachlan's molecular orbital (MO) calculation assuming $\theta\approx\phi$, the twisting angles (θ, ϕ) of the $2p_z$-*orbitals* on both α- and γ-allyl carbons were estimated to be about $28°$ for $\alpha,\alpha,\gamma,\gamma$-tetraphenyl allyl (TPA).[3]

Of particular interest is the fact that the methine-proton splitting of TPA shows a marked positive temperature dependence (Fig. 1). Carter *et al.*[7] interpreted the temperature-dependent splitting of the methylene proton in terms of the restricted rotation and a simple harmonic oscillator model based on the Stone-Maki theory.[8]

In order to explain the temperature dependence of the methine-proton splitting observed here, the detailed conformational analysis of these radicals is necessary. Hence, the electron-nuclear-double-resonance (ENDOR) and electron-spin-resonance (ESR) experiments have been carried out over a wide temperature range (from $-110°\mathrm{C}$ to $+210\ ^\circ\mathrm{C}$) in order to investigate the dynamic behavior of molecular motion. The most interesting result established by the ENDOR experiments at low temperatures is that the four phenyl groups in TPA are not equivalent
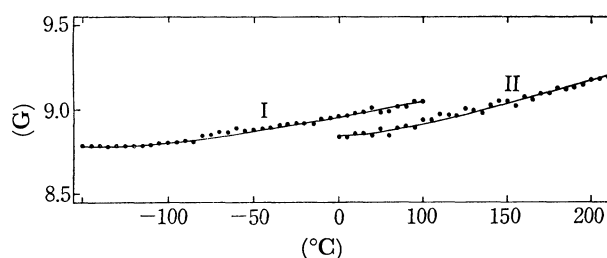

Fig. 1. Temperature dependence of the splitting constant A_β^H of TPA.

(I): in toluene, (II): in liquid paraffin.

each other, but are apparently to be classified into two different kinds of paired groups. On the other hand, the ESR results demonstrated that, in the higher-temperature region, the torsional vibration of the allyl skeleton $(\mathrm{C}\!\!=\!\!\mathrm{C}\!\!-\!\!)\mathrm{C} \rightleftarrows \mathrm{C}\!\!-\!\!(\mathrm{C}\!\!=\!\!\mathrm{C})$ becomes vigorous and the allyl skeleton begins to rotate internally. As the result, the four phenyl rings of TPA become almost equivalent because of the averaging effect of the rapid internal rotation of the allyl skeleton. These phenomena observed in the ESR spectra can be well treated by means of the following modified Bloch equation:[9,10]

$$G = \frac{i\omega_s M_0 \tau \sum\limits_{s=1}^{N} f_s}{N[1- \sum\limits_{s=1}^{N} f_s]} \tag{2}$$

where $f_s=(N+\alpha_s\tau)$, $\alpha_s=(1/T_{2s})-i(\omega_s-\omega)$, G: the complex transverse magnetization; ω_s: the resonance frequency for the species, s; M_0: the equilibrium value of polarization, M_z; τ: the mean life time; N: number of species; $1/T_{2s}$: transverse relaxation time, and ω: angular frequency. The results obtained from the computer simulation will be given in the following section. In this paper the author will report the results of the analyses of the temperature-dependent ESR and ENDOR spectra and will discuss in some detail the dynamic behavior of the molecular frameworks of the tetraaryl allyl radicals.

Experimental

The materials were TPA, α,α-diphenyl-γ,γ-dianisyl allyl (DPDAA), $\alpha,\alpha,\gamma,\gamma$-tetraanisyl allyl (TAA), α,α-diphenyl-γ,γ-diphenylene allyl (DDA), $\alpha,\alpha,\gamma,\gamma$-bisdiphenylene allyl (BDA), $\alpha,\alpha,\gamma,\gamma$-bisdiphenylene-$\beta$-azo allyl (BDAA), and $\alpha,\alpha,\gamma,\gamma$-bisdiphenylene-$\beta$-phenyl allyl (BDPA) (Fig. 2). They were prepared by following the process described in Refs. 11, 12, 13, 14, and 15.

(a)

(b)

(c)

(d)

(e)

(f)

(g)
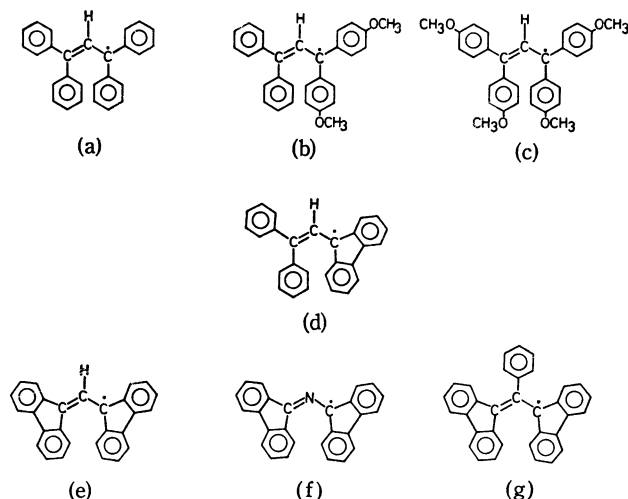
Fig. 2. Tetraaryl allyl radicals.
(a): TPA, (b): DPDAA, (c): TAA, (d): DDA, (e): BDA, f) BDAA, g): BDPA.

TPA: Found: C, 92.98; H, 5.58%. Calcd for $C_{27}H_{21}$: C, 93.86; H, 6.14%. DPDAA: Found: C, 85.56; H, 6.13%. Calcd for $C_{29}H_{25}O_2$: C, 85.89; H, 6.11%. TAA: Found: C, 79.76; H, 6.11%. Calcd for $C_{31}H_{29}O_4$: C, 79.98; H, 6.28%. DDA: mp 236.0—237.5 °C (235—237 °C).[12] BDA: mp 244.5—245.5 °C (245—246 °C).[13] BDAA: mp 270.0—271.5 °C (270—272 °C).[14] BDPA: Found: C, 94.65; H, 5.25%. Calcd for $C_{33}H_{21}$: C, 94.93; H, 5.07%.

The toluene and liquid paraffin used as solvents were well purified, dehydrated, and degassed. The ESR spectra were measured with a JEOL Model PE-3 X-band ESR spectrometer; an aqueous solution of peroxylamine disulfonate was used as standard of the magnetic field.[16] The ENDOR spectra were measured by means of a JEOL ES-EDX 1 spectrometer operating with a 80-Hz magnetic-field modulation in the temperature range from −110 to −40 °C for the toluene solutions and from 55 to 80 °C for the liquid paraffin solutions. The 150-watt CW RF field (6.5 KHz frequency modulation) was introduced into the coil inside the cavity for the NMR excitation. The hyperfine splitting constant was determined by averaging the values obtained from two or three measurements. The simulation of the spectra and the MO calculations were carried out at the Kyoto University Computer Center.

Results and Discussion

ENDOR Spectra.   Tetraphenyl Allyl-type Radicals: The ENDOR spectra of TPA, DPDAA, and TAA are shown in Fig. 3. It is obvious that the absorption lines near the free-proton frequency are due to the methoxy protons. The line at around 26 MHz was undoubtedly identified as the one due to the methine proton by reference to the ESR measurements. The two
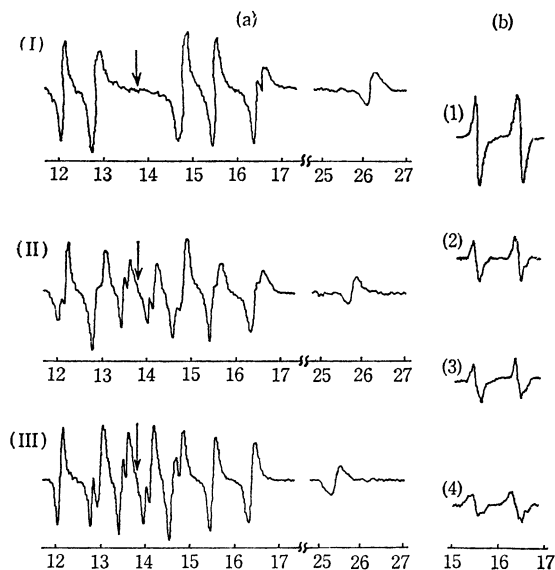

Fig. 3. ENDOR spectra of TPA-type radicals in toluene.
(a): at −80 °C: (I) TPA, (II) DPDAA, (III) TAA (b): temperature dependence of some lines of TAA 1) at −80 °C, 2) at −90 °C, 3) at −100 °C, 4) at −110 °C. Arrows: The position of the free proton frequency.
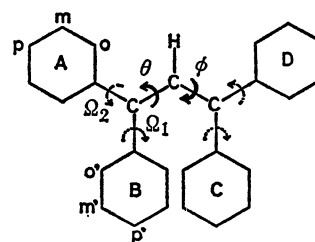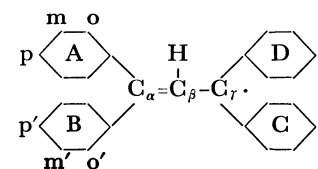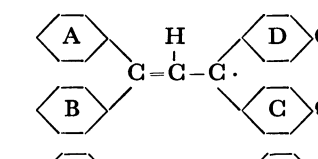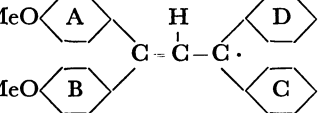

Fig. 4. Conformational model of TPA-type radicals.

lines at 15.5 MHz and 16.5 MHz for TAA are assumed to arise from the ortho-protons of the *interior* (**B**, **C**) and *exterior* (**A**, **D**) aryl groups respectively (see Fig. 4). From similar considerations, the absorptions at around 15.5 MHz and 16.5 MHz for TPA and DPDAA are attributed to the overlapping line arising from the ortho- and para-protons of the *interior* and *exterior* phenyl groups respectively. It should be remembered here that the ortho- and para-protons have hyperfine splitting constants of nearly the same magnitude, as is often the case with neutral aromatic free radicals.[17] The other absorptions observed at about 14.7 MHz are probably due to the meta-protons. The two kinds of hyperfine splitting constants observed for the methoxy protons in DPDAA and TAA imply that the methoxy-protons splitting constants on the *interior* rings are different from those on the *exterior* rings. This supports the previous assumption that the splitting of the ortho-proton of the *exterior* aryl groups is different from that of the *interior* groups. As has been described in a previous paper,[3] these tetraaryl allyl-type radicals have a twisted allyl skeleton, in which the distance between the rings of **B** and **C** (*interior* rings) is much closer than that between the rings of **A** and **D** (*exterior* rings) or of **A** and **B**. This model offers a reasonable theoretical basis for the present ENDOR experiments, in which a

TABLE 1. OBSERVED AND CALCULATED SPITTING

		α	β	γ	o(A)	m(A)	p(A)
(structure I)	Obsd.a) ESR		8.72		1.97	0.68	1.97
	ENDOR		8.808		1.911	0.697	2.043
	Calcd.b)	+0.318	9.142(1) / −0.099	+0.318	2.079 / +0.077	0.729 / −0.027	1.944 / +0.072
(structure II)	Obsd.a) ESR		≈9		S	S	S
	ENDOR		8.496		1.917	0.732	2.005
	Calcd.b)	+0.311	8.513(1) / −0.084	+0.295	2.052 / +0.076	0.648 / −0.024	1.971 / +0.073
(structure III)	Obsd.a) ESR		≈9		S	S	S
	ENDOR		8.234		1.876	0.731	0.247*
	Calcd.b)	+0.293	8.280(1) / −0.083	+0.293	1.836 / +0.068	0.567 / −0.021	0.056

S : Not confirmed. *: Methoxy proton. a) In toluene. b) Calculated splitting constants are obtained using the 50, $\theta = \phi = 28°$, where ρ_{Ci} are spin densities obtained by McLachlan's calculation using the following param-

nonequivalent spin distribution was observed between the *exterior* and the *interior* rings. This model also gives a good agreement between the observed and the calculated hyperfine splitting constants of the ring protons if one assumes $\theta = \phi = 28°$, $\Omega_1 = 35°$, and $\Omega_2 = 15°$ (see Fig. 4). Based on this model, the theoretical spin density on each carbon atom was calculated by means of McLachlan's MO method;[18] the results are given in Table 1, together with the hyperfine splitting constants calculated by the McConnell relation. The hyperfine splittings of the ring protons may be classified into three groups: the *ortho*- and *para*-protons of the *exterior* rings, those of the *interior* rings, and the *meta*-protons of all the rings. In the previous paper,[13] the four

phenyl rings of TPA were assumed to be nearly equivalent. However, it is more reasonable to assume the above-mentioned molecular structure (Fig. 4) in order to account for the ENDOR and the ESR spectra on the same basis.

Bisdiphenylene Allyl-type Radicals: Since BDA and BDAA are partially dimerized in a solution at low temperatures,[19] the ENDOR spectra of these radicals were not observed in toluene solutions in the temperature region suitable for this solvent. The ENDOR spectra for BDA, BDAA, and BDPA in liquid paraffin solutions are shown in Fig. 5. The smallest hyperfine splitting group of BDPA, which has never been observed in the ESR spectra, was clearly identified as being
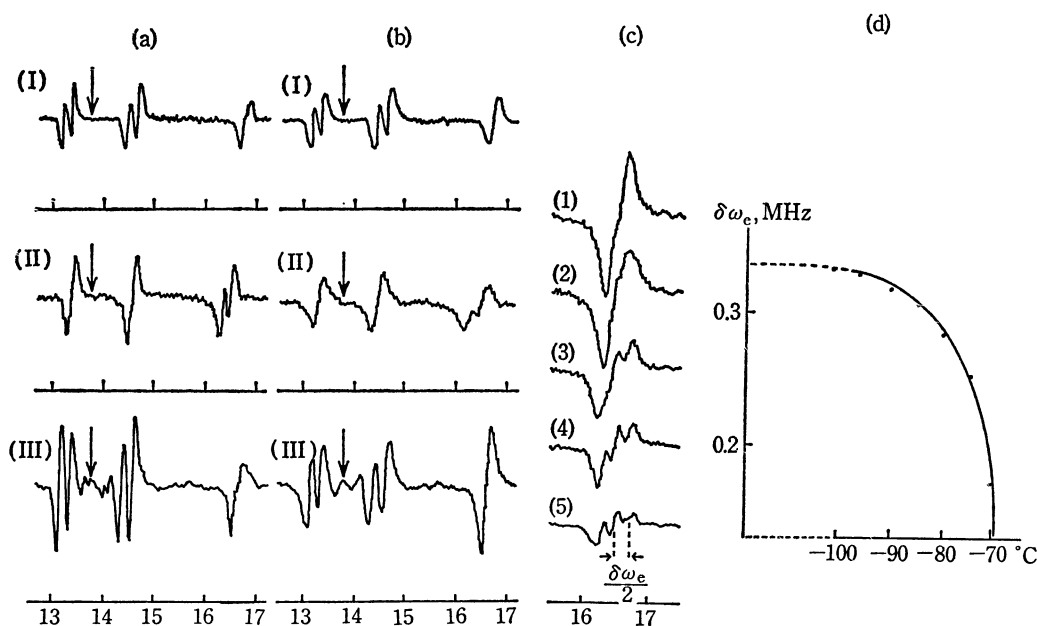

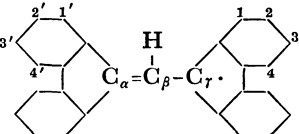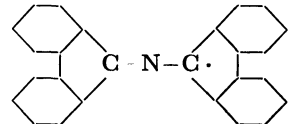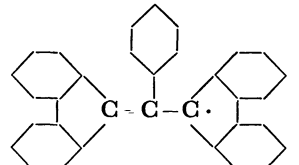Fig. 5. ENDOR spectra of BDA-type radicals in liquid paraffin.
(a): at 55 °C, (I) BDA, (II) BDAA, (III) BDPA, (b): at 80 °C, (I) BDA, (II) BDAA, (III) BDPA, (c): temperature dependence of some lines of BDPA in toluene 1) at −75 °C, 2) at −80 °C, 3) at −85 °C, 4) at −90 °C, 5) at −95 °C, (d): line separations of spectra (c). Arrows: The position of the free proton frequency.

CONSTANTS OF THE TPA-TYPE RADICALS (IN G)

o'(B)	m'(B)	p'(B)	o'(C)	m'(C)	p'(C)	o(D)	m(D)	p(D)
1.31	0.68	1.31						
1.240	0.697	1.240						
1.458	0.513	1.377						
+0.054	−0.019	+0.051						
S	S	S	S	S	S	S	S	S
1.303	0.596	1.303	1.193	0.596	0.168*	1.917	0.732	0.256*
1.458	0.486	1.404	1.269	0.459		1.809	0.594	
+0.054	−0.018	+0.052	+0.047	−0.017	+0.038	+0.067	−0.022	+0.054
S	S	S						
1.247	0.585	0.160						
1.296	0.432							
+0.048	−0.016	+0.040						

formula $A_{C_i}^H = |Q_{CH}^H| \cdot \rho_{C_i}$ $Q_{CH}^H = -27.0$ (i) $A_\beta^H = |Q_{CH}^H| \cdot \rho_{C\beta} + |B_{t-\pi}^H| \{\cos^2(90-\theta) \cdot \rho_{C\alpha} + \cos^2(90-\phi) \cdot \rho_{C\gamma}\}$, $|B_{t-\pi}^H| =$
eters $\lambda = 1.2$, $\alpha_{C-OMe} = \alpha + 0.5\beta$, $\beta_{C-OMe} = 0.6\beta$, $\theta = \phi = 28°$, $\Omega_1 = 35°$, and $\Omega_2 = 15°$.

TABLE 2. OBSERVED AND CALCULATED SPLITTING CONSTANTS OF THE BDA-TYPE RADICALS (IN G)

		α	β	γ	1,1'	2,2'	3,3'	4,4'
$C_\alpha=C_\beta-C_\gamma\cdot$	Obs.a) ESR		13.15		1.98	0.47	1.98	0.47
	ENDOR		S		2.008	0.520	1.956	0.388
	Calcd.b)		13.29[I]		1.890	0.324	1.593	0.054
		+0.262	−0.091	+0.262	+0.070	−0.012	+0.059	−0.002
$C-N-C\cdot$	Obs.a) ESR		3.40*		1.75	0.47	1.50	0.35
	ENDOR				1.782	0.437	1.564	0.396
	Calcd.b)		2.588[II]		1.809	0.324	1.539	0.054
		+0.253	−0.051	+0.253	+0.067	−0.012	+0.057	−0.002
$C-C-C\cdot$	Obs.a) ESR		S		1.96	0.67	1.96	0.67
	ENDOR		0.176** 0.095**		2.026	0.503	1.924	0.363
	Calcd.b)		1.890 −0.078		1.890	0.324	1.620	0.054
		+0.264		+0.264	+0.070	−0.012	+0.060	−0.002

S: Not confirmed. *: Splittings of nitrogen. **: Splittings of phenyl proton. a) In liquid paraffin. b) Calculated splitting constants are obtained using the formula $A_{C_i}^H = |Q_{CH}^H| \cdot \rho_{C_i}$, $Q_{CH}^H = -27.0$ (i) $A_\beta^H = |Q_{CH}^H| \cdot \rho_{C\beta} + |B_{t-\pi}^H| \{\cos^2$ $(90-\theta) \cdot \rho_{C\alpha} + \cos^2(90-\phi) \cdot \rho_{C\gamma}\}$, $|B_{t-\pi}^H| = 50$, $\theta = \phi = 37°$ (ii) $A_\beta^N = Q_1 \cdot \rho_{N\beta} + Q_2(\rho_{C\alpha} + \rho_{C\gamma})$, $Q_1 = +30.9$, $Q_2 = -2$, where ρ_{C_i} are spin densities obtained by McLachlan's calculation using the following parameters $\lambda = 1.2$, $\alpha_N = \alpha + 1.2\beta$, $\beta_{C-N} = 0.9\beta$, $\theta = \phi = 37°$, and in BDPA the tilted angle of the phenyl attached to the Cβ is assumed to be 30°.

due to the proton in the phenyl group attached to the β-carbon.[20,21] The multiple absorption lines at ca. 16.5 MHz vary as the temperature rises and collapse into a single line in the temperature region at around −65 °C, as is shown in Fig. 5-c. The proton hyperfine splitting constants thus obtained are shown in Table 2, where the assignment of the hyperfine splitting constants is based on the results of the MO calculations. From this table it may be seen that there are four kinds of equivalent protons in the biphenylene groups of each radical and that the splitting constants due to the corresponding protons in these radicals are almost equal.

In the BDA-type radicals, the two phenylene groups attached to the α- or the γ-carbon are fixed in the same plane and have no degree of free rotation, although this is not the case for the TPA-type radicals. Thus, if the two twisting angles of the allyl skeleton (θ and φ) were nearly equal, the spin-density distributions in the four aryl rings would be approximately equivalent. However, the temperature dependence of these ENDOR spectra (Fig. 5-c) indicates that the two twisting angles of the allyl skeleton will not be equal probably. On the other hand, the MO calculations show that if the difference in the two twisting angles (θ∼φ) is tentatively assumed to be 10°, the difference between $A_{1,3}^H$ and $A_{1',3'}^H$ is 0.5 G, while there is no noticeable difference between $A_{2,4}^H$ and $A_{2',4'}^H$. This result implies that the spectra which reflect the difference between θ and φ would be observed only at quite low tem-

peratures because of the torsional vibration of the allyl

skeleton $(C^{\theta}_{\cdot})C^{\phi}_{\cdot})C \rightleftarrows C^{\phi}_{\cdot})C^{\theta}_{\cdot})C)$.   However, this is not the case at ordinary temperatures because of the fast torsional vibration rate of the allyl skeleton. Thus, the several lines near 16.5 MHz collapse into a single line, while the two lines near 14.5 MHz remain unchanged, as is shown in Fig. 5. Similar phenomena were also observed in TPA-type radicals (Fig. 3-b). For such a temperature dependence of ENDOR spectra, Hyde et al.[22] used the Arrhenius equation rearranged as:

$$\log_{10} 1/\tau\delta\omega = \log_{10} 2\nu_0/\delta\omega - \Delta E/2.3RT \tag{3}$$

$$1/\tau\delta\omega = 2^{-1/2}[1 - (\delta\omega_e/\delta\omega)^2]^{1/2} \tag{4}$$

where τ is the lifetime of a proton in a particular site; $\delta\omega$, the separation of the two lines within the limits of slow exchange (assumed to be 0.34 MHz); ν_0, the frequency factor; ΔE, the activation energy of the torsional vibration of the allyl skeleton; R, the gas constant; T, the absolute temperature, and $\delta\omega_e$, the experimentally observed separation (Fig. 5-d). As an example, the Arrhenius plot obtained for BDPA from Eqs. (3), (4), and from the assumed value of $\delta\omega$, is shown in Fig. 6, from which the activation energy (ΔE) of the torsional vibration of the allyl skeleton

$(C^{\theta}_{\cdot})C^{\phi}_{\cdot})C \rightleftarrows C^{\phi}_{\cdot})C^{\theta}_{\cdot})C)$ is estimated to be about 2.5 kcal/mol. Judging from the fairly small magnitude of ΔE for the present radicals, the torsional vibration rate of the allyl skeleton may be very sensitive to the temperature variation.
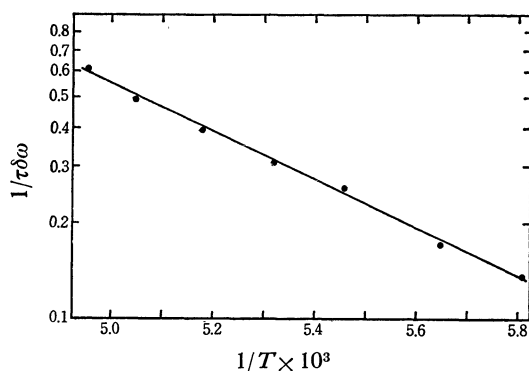

Fig. 6. Temperature dependence of the torsional vibration rate of the allyl skeleton of BDPA in toluene.

Temperature-dependent ESR Spectra and Molecular Dynamics.   Tetraphenyl Allyl: As Fig. 7 shows, the hyperfine structure of the ESR spectra of TPA changes markedly with the temperature. The spectra at low temperatures (Fig. 7a-1) were analyzed assuming the three non-equivalent hyperfine components ($A^H_{o,p}$, $A^H_{o',p'}$, and $A^H_{m,m'}$), as has been established by the ENDOR measurements. The hyperfine splitting constants thus determined are listed in Table 3. As the temperature increases, the spectral pattern changes remarkably; at around 115 °C (Fig. 7a-3) it becomes a seven-line pattern with the line separation of ($A^H_{o,p}$ + $A^H_{o',p'}$). This hyperfine pattern can be interpreted in terms of a typical line-width alternation, as has
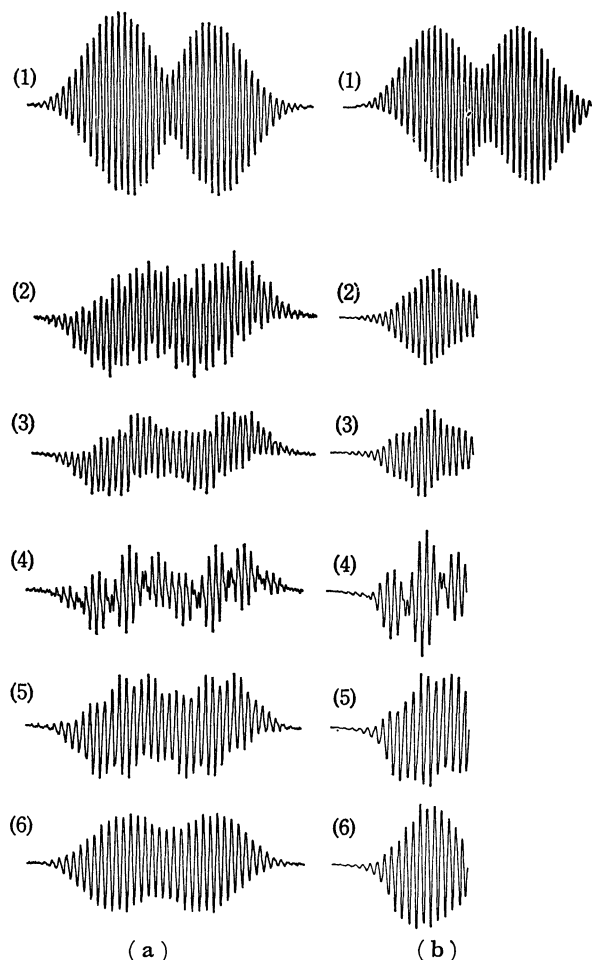

Fig. 7. Temperature-dependent ESR spectra of TPA in liquid paraffin.

(a): Observed spectra 1) at −80 °C in toluene, 2) at 55 °C, 3) at 90° C, 4) at 115 °C, 5) at 140 °C, 6) at 170 °C

(b): Simulated spectra 1) obtained by ENDOR result at −80 °C in toluene ($\tau = \infty$), 2) $\tau = 1.0 \times 10^{-6}$, 3) $\tau = 6.0 \times 10^{-7}$, 4) $\tau = 2.0 \times 10^{-7}$, 5) $\tau = 6.0 \times 10^{-8}$, 6) $\tau = 4.0 \times 10^{-8}$

TABLE 3.   HYPERFINE SPLITTING CONSTANTS OF TPA IN LIQUID PARAFFIN SOLUTION (IN G)

Temperature (°C)	method	A^H_β	$A^H_{o,p}$	$A^H_{o',p'}$	$A^H_{m,m'}$
+ 55	ENDOR	8.810	2.011 1.894	1.166	0.692
	ESR	8.86	1.95	1.22	0.67
+110	ESR	8.97	3.08/2	3.08/2	0.70
+170	ESR	9.10	1.45	1.45	0.70

been discussed in the Introduction, and its intensity ratio coincides well with that to be expected from the theory for an extremely broadened case (the doublet of 1 : 36 : 225 : 400 : 225 : 36 : 1). The line-width alternation effect observed here may be attributed to the exchange of the *interior* and *exterior* rings due to the internal rotation of the allyl skeleton of TPA, shown in Fig. 8. At low temperatures, the rate of the internal rotation is slow, and the $A^H_{o,p}$ and $A^H_{o',p'}$

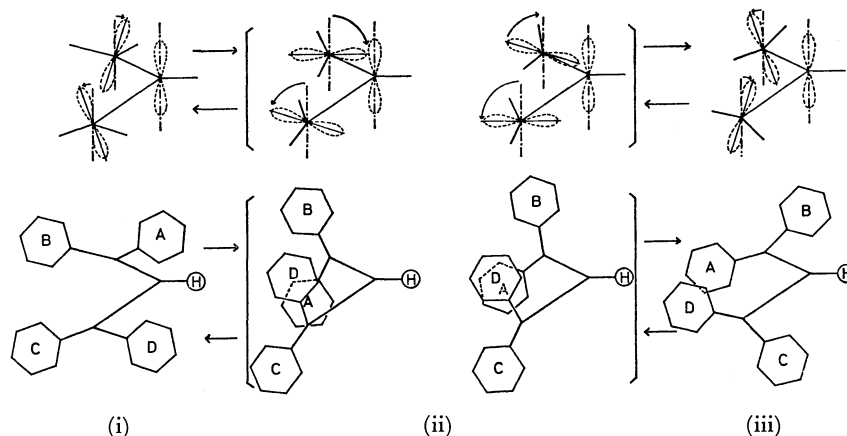(i)   (ii)   (iii)

Fig. 8. Model of the internal rotation of the allyl skeleton.
Here, the interchange between the tilted angles of phenyl rings (Ω_1, Ω_2) is also considered to take place cooperative with the internal rotation of the allyl skeleton.
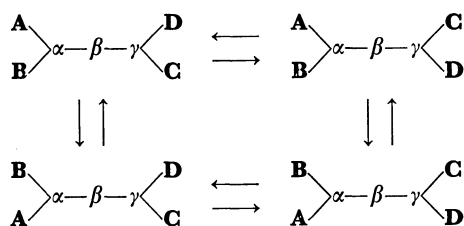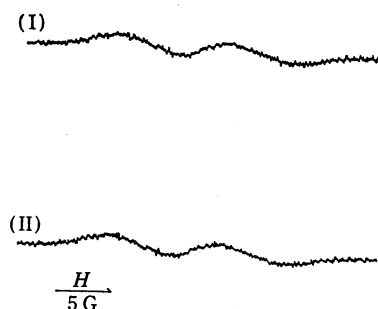
values are separately observed. At higher temperatures, however, the internal rotation is so rapid that it is not possible to distinguish the interior-phenyl protons from the exterior-phenyl ones because of the rapid exchange between the two states. This rate process may be analyzed by using a modified Bloch equation for the two-jump model*. The computer-simulated ESR spectra obtained on the basis of this model are compared with the observed spectra in Fig. 7. Here, the small temperature changes in the hyperfine splitting constants were ignored and the hyperfine splitting constants determined by the ENDOR measurements were used as those at the limit of the slow exchange rates. By applying the estimated lifetime (τ) to the following Arrhenius relation, the activation energy, Ea, of the internal rotation was evaluated:

$$k = 1/\tau = k_0 \exp \left(-Ea/RT\right), \qquad (5)$$

where k is the rate constant of the internal rotation, and k_0, the frequency factor. A plot of $\log_{10} 1/\tau$ against $1/T$ is shown in Fig. 9, from which Ea and k_0 were calculated to be 13.4 kcal/mol and 2.3×10^{14} s^{-1} respectively.

DPDAA and TAA showed merely broadened ESR spectra, as is shown in Fig. 10. The reason why these spectra do not split more clearly may owe to the unresolved small hyperfine splittings of the methoxy protons. This reasoning was confirmed by the ENDOR measurements. If these ESR spectra were well-resolved, the line-width alternation effects would be

---

* Strictly speaking, the internal rotation of the allyl skeleton must be expressed by the following four-jump model:

However, since only the two kinds of interconversion at the sites of α and γ are expected to be cooperative, it seems to be enough to assume merely the two-jump model.

1/T × 10³

Fig. 9. Plots of $\log_{10} 1/\tau$ against $1/T$ 10^3.
(I): for TPA ●, (II) for DDA ○.

Fig. 10. ESR spectra of DPDAA (I) and TAA (II) at −85 °C in toluene.

observed as well.

Bisdiphenylene Allyl: As is shown in Fig. 11, the hyperfine patterns of the ESR spectra of BDA are not temperature-dependent. Each phenylene ring of BDA has no degree of free rotation; therefore, there may be little difference between the interior and exterior proton splittings in the biphenylene group. This was confirmed by the results of the ENDOR measurements. Because of the equivalency of the two kinds of the
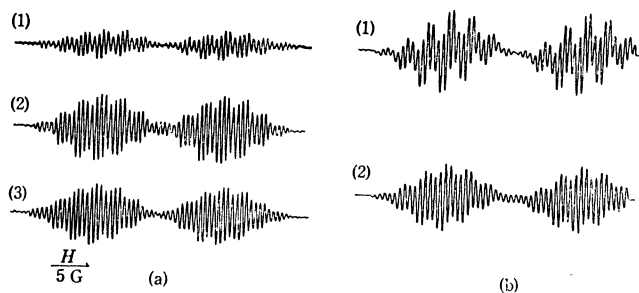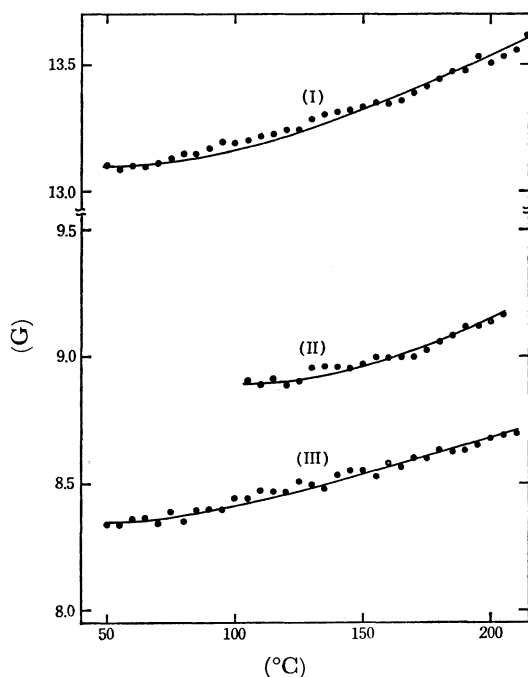
Fig. 11. ESR spectra of BDA in liquid paraffin.
(a): Observed spectra 1) at 55 °C, 2) at 115 °C, 3) at 215 °C, (b): Simulated spectra 1) obtained by ENDOR result at 55 °C, 2) obtained by ESR result at 55 °C.

Fig. 12. Temperature dependence of the splitting constant A_{β}^{H}.

(I): BDA, (II): DDA, (III): TPA

TABLE 4. HYPERFINE SPLITTING CONSTANTS OF DDA IN LIQUID PARAFFIN SOLUTION (IN G)

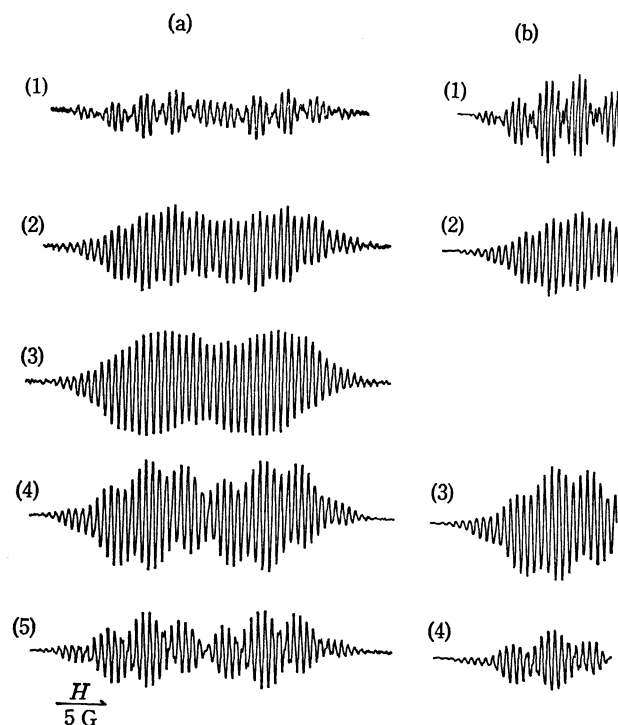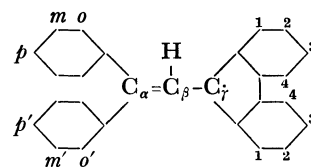| Temperature (°C)	A_{β}^{H}	$A_{1,3}^{H}$	$A_{o,p}^{H}$	$A_{o',p'}^{H}$	$A_{2,4}^{H}$	$A_{m,m'}^{H}$
+110	9.39	2.44	2.44	1.10	0.55	0.55
+150	9.46	S	S	S	0.55	0.55
+190	9.52	2.90	1.65	1.65	0.55	0.55

S not confirmed

Fig. 13. Temperature-dependent ESR spectra of DDA in liquid paraffin.
(a): Observed spectra 1) at 110 °C, 2) at 130 °C, 3) at 145 °C, 4) at 180 °C, 5) at 200 °C
(b): Simulated spectra 1) $\tau = 5.0 \times 10^{-6}$, 2) $\tau = 2.5 \times 10^{-6}$, 3) $\tau = 8.0 \times 10^{-8}$, 4) $\tau = 5.0 \times 10^{-8}$

aryl rings in BDA, there is no line-width alternation effect in the ESR hyperfine pattern. However, the slope of the plots of the A_{β}^{H} vs. temperature (Fig. 12) is similar to that for TPA. This suggests that the internal rotation of the allyl skeleton might also take place in BDA, as will be discussed later.

Diphenyl Diphenylene Allyl: The ENDOR spectrum of this radical has not been observed; therefore, its hyperfine splitting constants were analyzed with reference to the analyses of the observed ESR spectra for BDA and TPA. From the result of the computer simulation, the hyperfine splitting constants of the proton of DDA were assigned as shown in Table 4. The increase in $A_{1,3}^{H}$ with the temperature shows that the delocalization of an odd electron to the biphenylene group may be more favorable than that to the two phenyl rings, because with a rise in the temperature the conjugation of the biphenylene group with the allyl framework may become more favorable than that of the

two phenyl rings, which undergo restricted rotation. Furthermore, at low temperatures evidences were obtained for inequivalent phenyl rings (interior and exterior) in DDA, while, on warming, the allyl skeleton begins to rotate internally. Hence, the interconversion between the two phenyl rings must be the origin of the complex temperature dependence of the ESR spectral pattern shown in Fig. 13. Therefore, the two-jump model was tentatively applied in the manner described for TPA. The activation energy for an interconversion of the two phenyl rings (=internal rotation of the allyl skeleton) thus estimated is about 22.3 kcal/mol, and the frequency factor (k_0), about 1.4×10^{19} s^{-1} (Fig. 9).

Temperature Dependence of A_{β}^{H}. The temperature dependence of A_{β}^{H} of TPA is shown in Fig. 1.

The slopes of the plots of the A_β^H vs. the temperature at high temperatures are nearly independent of the solvents. In addition, the ESR hyperfine patterns of toluene solutions at 90—100 °C are essentially the same as those of liquid paraffin solutions at 115—135 °C. This suggests that the temperature dependence of A_β^H is caused by the intramolecular dynamics of the allyl skeleton. Similar results were obtained for both BDA and DDA, as is shown in Fig. 12. The observed A_β^H at lower temperatures are likely to be constant. This is related to the fact that the torsional vibration of the allyl skeleton is very slow at very low temperatures, as was confirmed by the ENDOR analyses of the BDA-type radicals. At such temperatures, the internal rotation of the allyl skeleton does not take place; also, the two twisting angles of the allyl skeleton are different from each other. As the allyl skeleton begins to rotate internally with a rise in the temperature, the two $2p_z$-orbitals on both the α and γ carbon atoms tend to overlap with the 1s-orbital of the methine proton (Fig. 8). Hence, A_β^H must reach a maximum in the state of Fig. 8-(ii)**. When the internal rotation rate is slow (that is, when the τ-values are large), the probability of finding the state of Fig. 8-(ii) may be small, resulting in a small A_β^H. On the other hand, when the internal rotation becomes faster (that is, when the τ-values are smaller), the probability of finding the state of Fig. 8-(ii) may increase, making A_β^H larger and larger.

Conclusion

1. At low temperature the allyl skeleton of the tetraaryl allyl radicals oscillates very slowly.

2. The torsional vibration becomes larger with an increase in the temperature, and the allyl skeleton begins to rotate internally at high temperatures.

3. Line-width alternation effects have been observed in TPA and DDA, the activation energies of their internal rotations being 13.4 kcal/mol and 22.3 kcal/mol respectively.

4. The temperature dependence of A_β^H is interpreted by means of the mechanism of the internal rotation of the allyl skeleton.

** Here, the author assumes that an odd electron distribution on the allyl skeleton is kept almost constant with temperature variation. (cf. sections of TPA and BDA)

References

1) G. R. Luckhurst, Mol. Phys., 11, 205 (1966).

2) A. Berndt, Tetrahedron, 25, 37 (1969).

3) K. Watanabe, J. Yamauchi, H. Ohya-Nishiguchi, Y. Deguchi, and H. Takaki, This Bulletin, 45, 371 (1972).

4) C. Heller and H. M. McConnell, J. Chem. Phys., 32, 1535 (1960).

5) R. W. Fessenden and R. H. Shuler, ibid., 39, 2147 (1963).

6) W. A. Forbes, P. D. Sullivan, and H. M. Wang, J. Amer. Chem. Soc., 89, 2705 (1967).

7) M. K. Carter and G. Vincow, J. Chem. Phys., 47, 302 (1967).

8) E. W. Stone and A. H. Maki, ibid., 37, 1326 (1962).

9) J. H. Freed and G. K. Fraenkel, ibid., 39, 326 (1963).

10) P. D. Sullivan and J. R. Bolton, "Advances in Magnetic Resonance," Vol. 4, ed. by J. S. Wangh, Academic Press, New York, N. Y. (1970), p. 39.

11) K. Ziegler, Ann. Chem., 434, 34 (1932).

12) R. Kuhn and D. Rewicki, ibid., 690, 50 (1965).

13) R. Kuhn, H. Fischer, F. A. Neugebauer, and H. Fischer, ibid., 654, 64 (1962).

14) R. Kuhn and F. A. Neugebauer, Monatsh. Chem., 94, 16 (1963).

15) R. Kuhn and F. A. Neugebauer, ibid., 95, 3 (1964).

16) G. E. Pake, J. Townsend, and S. I. Weissman, Phys. Rev., 85, 683 (1952).

17) A. H. Maki, R. D. Allendoerfer, J. C. Danner, and R. T. Keys, J. Amer. Chem. Soc., 90, 4225 (1968).

18) A. D. McLachlan, Mol. Phys., 3, 233 (1960).

19) K. Watanabe, J. Yamauchi, H. Ohya-Nishiguchi, and Y. Deguchi, This Bulletin, 47, 274 (1974).

20) K. Watanabe, J. Yamauchi, H. Ohya-Nishiguchi, Y. Deguchi, and K. Ishizu, Chem. Lett., 1974, 489.

21) N. S. Dalal, D. E. Kennedy, and C. A. McDowell, J. Chem. Phys., 61, 1689 (1974).

22) J. H. Hyde, R. Breslow, and C. DeBoer, J. Amer. Chem. Soc., 88, 4763 (1966).